CONF-750908--4

STRUCTURAL ANALYSIS TECHNOLOGY FOR HIGH-TEMPERATURE DESIGN*

W. L. Greenstreet
Holifield National Laboratory
Oak Ridge, Tennessee 37830

Results from an ongoing program devoted to development of a verified high-temperature structural design technology are described. This technology embraces design methods and criteria applicable to inelastic behavior of reactor system components under time-varying temperature and load conditions. The major aspects addressed by the program are (1) deformation behavior; (2) failure associated with creep rupture, brittle fracture, fatigue, creep-fatigue interactions, and crack propagation; and (3) the establishment of appropriate design criteria.

This paper discusses information developed in the deformation behavior category, which includes studies of materials behavior; development of mathematical analogs, or constitutive equations, to describe this behavior; and the development and assessment of structural analysis methods. The material considered is type 304 stainless steel, and the temperatures range to 1100°F (593°C).

First, results obtained through uniaxial tests to study elastic-plastic, creep, and relaxation behaviors are described. Results from specialized tests for examining various loading history aspects along with combined stress test results are also included. These data were obtained as a part of relatively long-term efforts to provide experimental bases for the development of constitutive equations which realistically model nonlinear hereditary mechanical behavior.

Constitutive equations identified and developed for interim use in design analyses are then discussed. Since the equations were to fill current and near-term needs existing knowledge in the constitutive equation area, current computational methods and capabilities, and mechanical property data requirements entered into the equation recommendations. In addition, small deformation behavior was assumed to prevail in application, and it was postulated that the total strain tensor could be decomposed into time-independent (elastic and plastic) components and time-dependent (creep) components. Thus, constitutive equations were considered for each type of deformation.

The constitutive equations were incorporated into finite-element computer codes developed under the overall program. Results from two computer codes, a research type and a special-purpose type, for treating plane and axisymmetric structures are compared with experimental data. The latter were obtained from beam and plate specimens tested at 1100°F (593°C) and from a straight-pipe specimen tested at temperatures varying from 800 to 1100°F (427 to 593°C). The beam and plate specimens were simply supported and subjected to concentrated force loadings at the center. Fully reversed cyclic loadings were employed. The straight-pipe specimen was subjected to internal pressure and thermal transient loadings. The maximum temperature was 1100°F (593°C), and the thermal transients were induced by flowing sodium inside the

*Research sponsored by the Energy Research and Development Administration under contract with Union Carbide Corporation.

specimen; the combination of pressure and transient loadings produced ratchetting. Generally good agreement between calculated and experimental results was obtained for each specimen type.

In essence, the paper considers the ingredients necessary for predicting relatively high-temperature inelastic deformation behavior of engineering structures and gives some examples. These examples illustrate the utility and acceptability of the computational methods identified and developed for predicting essential features of complex inelastic behaviors. Conditions and responses that can be encountered under nuclear reactor service conditions are invoked in the examples.

42

End of the text

References

References

1. C. E. Pugh, K. C. Liu, J. M. Corum, and W. L. Greenstreet, "Currently Recommended Constitutive Equations for Inelastic Design Analysis of FFTF Components," USAEC Report ORNL-TM-3602, September 1972.

2. J. M. Corum, W. L. Greenstreet, K. C. Liu, C. E. Pugh, and R. W. Swindeman, "Interim Guidelines for Detailed Inelastic Analysis of High-Temperature Reactor System Components," USAEC Report ORNL-5014, December 1974.

3. J. M. Corum and W. K. Sartory, "Elastic-Plastic Creep Analysis of Thermal Ratchetting in Straight Pipe and Comparisons with Test Results," ASME Paper 73-WA/PVP-4.

1. Introduction

A continuing challenge is that of understanding and predicting inelastic behaviors of metal structures under complex loading conditions. In recent years, this challenge has been heightened by requirements imposed by the design of Liquid-Metal Fast Breeder Reactor (LMFBR) components and systems. The relatively high operating temperatures, the very good heat transfer characteristics of the sodium coolant, the long design lifetimes, and the safety, reliability, and operability demands combine to require detailed examinations of inelastic behaviors of the structures involved. Clearly, the mechanical behaviors of the materials of construction must be understood and the inherent capabilities of these materials utilized to the fullest extent possible commensurate with good practice.

This paper discusses the ingredients associated with inelastic analyses for predicting deformation behaviors and describes the technology currently available and in use by LMFBR design analysts. These ingredients include mechanical behavior information on the materials of construction, constitutive equations to mathematically describe these behaviors, and certified structural analysis methods and tools. Each is addressed in the sections below.

2. Mechanical Behavior

In this paper, we restrict our discussion to type 304 stainless steel; the temperatures of interest range up to about 1100°F (593°C). Materials from a single reference heat of type 304 stainless steel was used in obtaining all mechanical property and structural test data described in this paper, except those shown in Figs. 1(b-1), 3(b), and 4(a) to be discussed later. Material from a second heat was used in these ~~two~~ three cases. All specimens were given

identical pretest heat treatments, that is, a full anneal at 2000°F (1093°C) for 30 minutes.

To illustrate the short-time behavior of the material, stress-strain results from tensile tests at various temperatures are shown in Fig. 1(a), while curves obtained from cyclic loading between fixed strain limits are shown in Fig. 1(b). The pronounced increase in deformation resistance, or hardening, of this material with increased plastic deformation can be seen in Fig. 1(b) for two temperature levels. However, hardening and hardening retention are influenced by several factors. While accumulated plastic strains increase hardening, such conditions as hold times at zero stress and high temperature, periods of creep, and periods of relaxation can reduce it.

Combined-stress tests of thin-walled cylindrical specimens, which were subjected to axial and torsional loads, were used to obtain data on yield surface behavior. The stress corresponding to approximately 10 μ-in. (25.4 μ-mm) offset strain was defined as the yield stress in this case. A yield locus obtained at room temperature and subsequent yield curves associated with prestressing along straight-line loading paths are shown for one tubular specimen in Fig. 2(a). The subsequent loci correspond to the prestressing points indicated by the crosses. Note that the prestressing points are generally outside the corresponding yield loci. The von Mises formulation gives good descriptions of initial yield surfaces as shown; these surface move and change in size and shape with plastic deformation.

The lower part of Fig. 2 shows subsequent yield surfaces at various temperatures. To obtain these results, a thin-walled cylindrical specimen was heated to 500°F (260°C) and prestressed to the point P shown in the first diagram. Yield loci were then determined sequentially at each of the lower temperatures indicated, except for the first prestressing case. In this case,

after the 500°F (260°C) curve (dashed) was obtained and the temperature was reduced to 350°F (177°C) the specimen was unintentionally loaded to point Q. Hence, the procedure was reinitiated by moving the stress point to near the center of the elastic region and again heating to 500°F. Note that the two 500°F curves in the first diagram are not markedly different, but the 500°F curves were the most significantly affected by subsequent changes in prestressing. The yield curves at the higher temperatures were enclosed by those at the lower temperatures for each of the three prestressing cases (maximum total strain of ≥ ___ %).

Time-dependent behavior of type 304 stainless steel is illustrated by the creep strain versus time results from constant-load constant-temperature tests shown in Fig. 3. Step-load, cyclic-load, and relaxation test results are shown in Fig. 4. The data in Fig. 4(a) are from step-increased-load tests, while Fig. 4(b) and 4(c) show the cyclic load behavior, where the first half cycle is in tension in one case and in compression in the other.

Combined-stress loading creep behavior was also examined using thin-walled cylindrical specimens, which were subjected to axial force and torsional moment loadings. Data obtained by Findley [1] from a 1000-hr, 1100°F (593°C) test in which the axial stress was 10.63 ksi (73.29 MPa) and the torsional stress was 6.11 ksi (42.13 MPa) are shown in Fig. 5. A constant ratio of the strains with time is seen in Fig. 5(a), while Figs. 5(b) and (c) depict the axial and torsional responses, respectively.

3. Constitutive Equations

Continuing research is in progress to characterize material behaviors and to derive constitutive equations which realistically describe the complex hereditary nonlinear mechanical behaviors exhibited. To meet existing design needs, constitutive equations were identified and developed for interim use. The resultant recommendations were based on combined considerations of existing

knowledge in the constitutive equation area, current computational methods and capabilities, and mechanical property data requirements.

Small deformation behavior was assumed to prevail in application, and it was postulated that the total strain tensor could be decomposed into time-independent (elastic and plastic) components and time-dependent (creep) components. Thus, constitutive equations were considered for each type of deformation. Classical kinematic hardening theory (Prager [2], Shield and Zeigler [3], and Zeigler [4]) was recommended (Pugh et al. [5] and Corum et al. [6]) for use in describing elastic-plastic behaviors of stainless steels. This theory provides acceptable representations of essential features of the observed behavior; its use is compatible with computational methods currently employed and with the existing materials data base. The classical theory was modified along lines described by Prager [7] to account for temperature effects, and auxiliary rules were provided to account for, in an approximate way, additional influences of deformation history on subsequent deformation response.

A equation-of-state-type formulation was adopted (Pugh et al. [5] and Corum et al. [6]) for use in expressing creep strain rates (both primary and secondary) in terms of applied stresses and other variables. This selection represented a logical choice for near-term use when the availability of relevant information on creep behavior and of required data for current use in design analyses were considered. Through comparison with experimental data, the strain hardening rule (Robotnov [8] and Odqvist [9]) was selected to represent responses under changing stress conditions. However, since the usual strain-hardening procedure does not apply in cases of stress reversals, auxiliary rules were also provided to remove this deficiency.

To complete the examination of elements for multiaxial creep formulations, several expressions for representing creep strains under constant uniaxial stress and temperature conditions were studied. Candidate equations are shown

in Fig. 3(b). The first employs two exponential terms to describe primary creep strains, while the other two equations contain single-term representations. Because the first equation gives good fits to experimental data at both short and long times, it was selected for design use. However the second equation was used to obtain calculated responses which are described later in this paper.

Comparisons between computed and measured results for the uniaxial case are given in Fig. 4(a) (predictions shown as solid curves), Figs. 4(b) and (c) (dashed curve segments), and in Fig. 4(d) (dashed curve). The predictions in the cyclic creep and relaxation cases [Figs. 4(b) through 4(d)] were made on the basis of the single-exponential-term creep equation and data from a group of uniaxial, constant-load creep tests on specimens taken from the same plate of material. The overall agreement is good for the conditions examined. Differences between predicted and measured results stem, at least in part, from lack of agreement in uniaxial test results and from a less than adequate representation, given by the equation selected, of the very steep portion of the uniaxial creep response at the stress levels and very short times of interest.

Calculated and measured results are compared for the combined stress case in Figs. 5(b) and (c). Reasonable agreement between results is exhibited in each of these figures.

4. Analysis of Inelastic Structural Response

Structural analysis methods capable of incorporating the constitutive equations and treating geometries and loadings of interest complete the compliment of tools needed. To indicate accuracies of results obtained in the analysis of structures, a simply-supported, center-loaded, circular plate (CP4) is considered. The plate was 20.75 in. (~~52.71 cm~~ 0.527 m) in outside diameter and 0.5 in. (~~1.27 cm~~ 12.7 mm) thick. It was loaded by a concentrated force applied through a boss

at the center and supported on a 20.0 in. (~~50.8 mm~~ 0.508 m) diameter circle. The test temperature was 1100°F (593°C); deflection control was employed, with maximum center deflections being ±0.11 in. (±2.79 mm).

A special-purpose type finite element computer code, CREEP-PLAST (Clinard and Crowell [10]), which was developed under the overall program was used in the structural analysis. This code treats two-dimensional (plane and axisymmetric) structures, employs 3-node triangular elements (two degrees of freedom at each node) and uniaxial bar elements, and incorporates the recommended constitutive equations and auxiliary calculational procedures. In the analysis, a symmetry section of one-half of the plate was represented by a mesh of 748 axisymmetric revolved triangular elements, giving 928 degrees of freedom. Bilinear representations of stress-strain response were based on cyclic curves for a strain range of 0.4%; the tenth cycle representation was used for all plastic loadings subsequent to the first.

The loading history in terms of center deflection versus time is shown in Fig. 6(a) for plate specimen CP4. Key points on the diagram are numbered for reference in the other plots of the figure. The measured and predicted load versus center deflection behaviors for "instantaneous" load changes from points 1 to 2, 3 to 4, and 5 to 6 are shown in Fig. 6(b). The agreement is reasonably good, with the calculated maximum load being somewhat greater than the measured value for each deflection change segment.

The predicted and measured loads during the two hold periods at maximum deflection are shown in Fig. 6(c), that is, for the hold (relaxation) periods from 2 to 3 and from 4 to 5. The calculated loads at the ends of the hold periods are in much better agreement than at the beginnings of these periods. The overall descrepancies reflect inadequacies in uniaxial creep response representation as mentioned in the previous section. Finally, comparisons of

results for the ten short-time cycles [6 to 7 in Fig. 6(a)] imposed after the second period of relaxation are shown in the load-deflection plot of Fig. 6(d). Note that the curves are plotted from the deflection at zero load. The deformation resistance of the material was less than predicted, giving larger loads under positive deflection portions of the cycles than measured. However, the shakedown prediction was good.

Similar agreement was obtained for a simply-supported rectangular beam loaded at the center and tested in the deflection control mode. For load-control situations the agreement, although reasonable, is generally not as good largely because the results are more sensitive to discrepencies in stress-strain response representations. Very good agreement was obtained between predicted and measured results from a test in which a pipe specimen (Corum and Sartory [11]) was subjected to complex thermal and mechanical loadings to simulate nuclear reactor service conditions.

5. Conclusions

The results given indicate the state-of-the-art of inelastic structural analysis methodology that is available for general use by design analysts. Despite needs for additional research and development work, essential features of inelastic behaviors of structures under complex time-varying loading conditions can be predicted with reasonable accuracy, giving rational bases for design guidance and performance assessments.

Acknowledgements

My sincere appreciation is extended to the following persons for information contained in this paper: to J. M. Corum and J. A. Clinard for structural analysis and test data; to K. C. Liu and C. E. Pugh for constitutive equation development information; and to R. W. Swindeman for mechanical properties data.

References

[1] FINDLEY, W. N., "Multiaxial Creep Studies", High-Temperature Structural Design Methods for LMFBR Components Quart. Prog. Rep. for Period Ending June 30, 1972, ORNL-TM-3917, pp. 10-25.

[2] PRAGER, W., "The Theory of Plasticity: A Survey of Recent Achievements (James Clayton Lecture)", Proc. Inst. Mech. Eng. 169 pp. 41-57 (1955).

[3] SHIELD, R. T. and ZIEGLER, H., "On Prager's Hardening Rule", Z. Ang. Math. Phys. IXA pp. 260-276 (1958).

[4] ZIEGLER, H., "A Modification of Prager's Hardening Rule", Quart. Appl. Math. 17 pp. 55-65 (1959).

[5] PUGH, C. E. et al., "Currently Recommended Constitutive Equations for Inelastic Analysis of FFTF Components", ORNL-TM-3602 (September 1972).

[6] CORUM, J. M. et al., "Interim Guidelines for Detailed Inelastic Analysis of High-Temperature Reactor System Components", ORNL-5014 (December 1974).

[7] PRAGER, W., "Non-Isothermal Plastic Deformation", Proc. Koninklijke Nederlandsche Akademie van Wetenschappen 61, (3B) pp. 176-182 (1958).

[8] ROBOTNOV, Yu N., Creep Problems in Structural Members, pp. 206-207, American-Elsevier Publishing Co., Inc., New York, 1969.

[9] ODQVIST, F. K. G., "Non-Linear Solid Mechanics-Part, Present, and Future", Proc. Twelfth Int. Conf. on Appl. Mech., Stanford University, August 26-31, 1968, pp. 77-99, Springer-Verlag, New York (1969).

[10] CLINARD, J. A. and CROWELL, J. S., "ORNL User's Manual for CREEP-PLAST Computer Program", ORNL-TM-4062 (November 1973).

[11] CORUM, J. M. and SARTORY, W. K., Elastic-Plastic Creep Analysis of Thermal Ratchetting in Straight Pipe and Comparisons with Test Results, ASME Paper No. 73-WA/PVP-4, 1973.

List of Figures

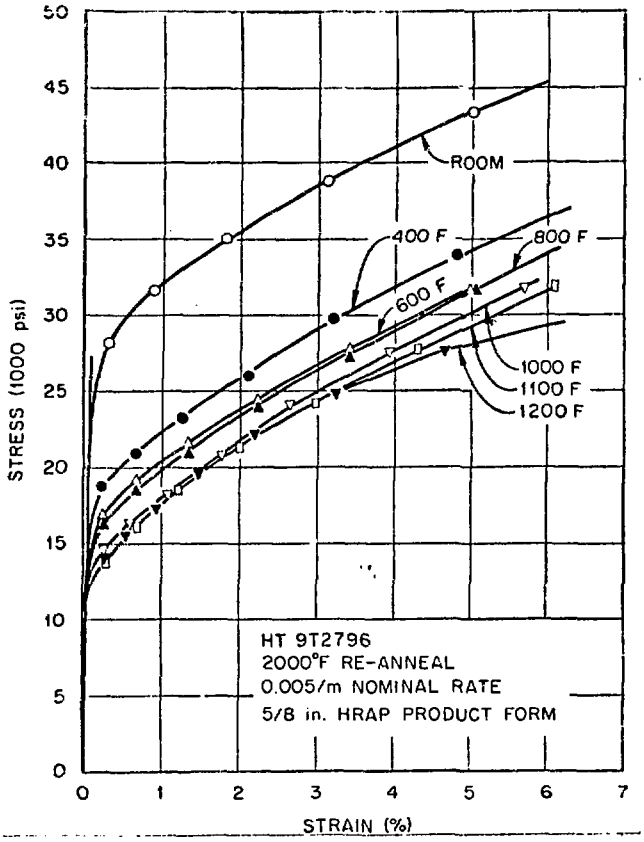

TYPE 304 STAINLESS STEEL, ANNEALED (HEAT 8043813)
ROOM TEMPERATURE
STRAIN RATE 0.005/min
STRAIN RANGE ≈ 0.9%

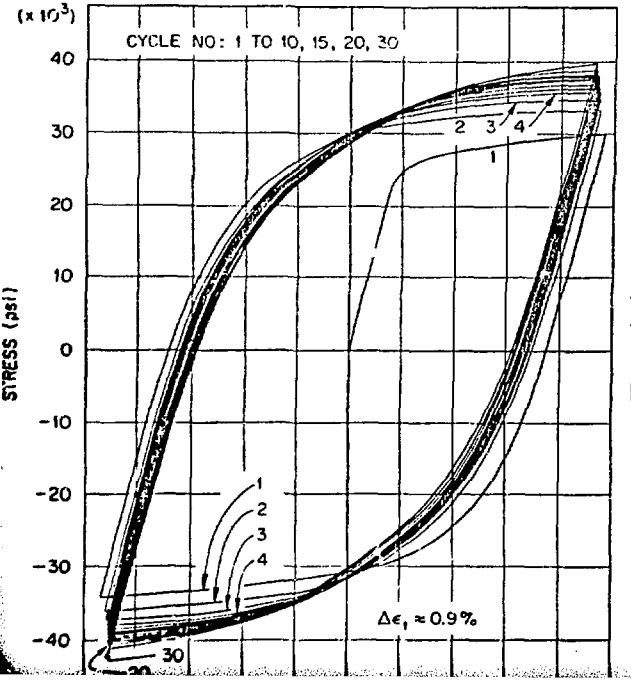

TYPE 304 STAINLESS STEEL, ANNEALED (HEAT 9T2796)
TEMPERATURE 1100°F
STRAIN RATE 0.005/min
STRAIN RANGE 1.0%

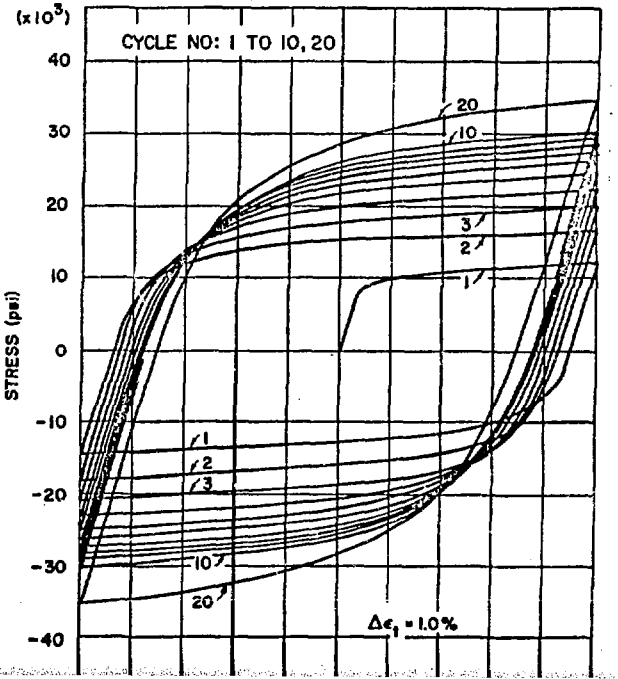

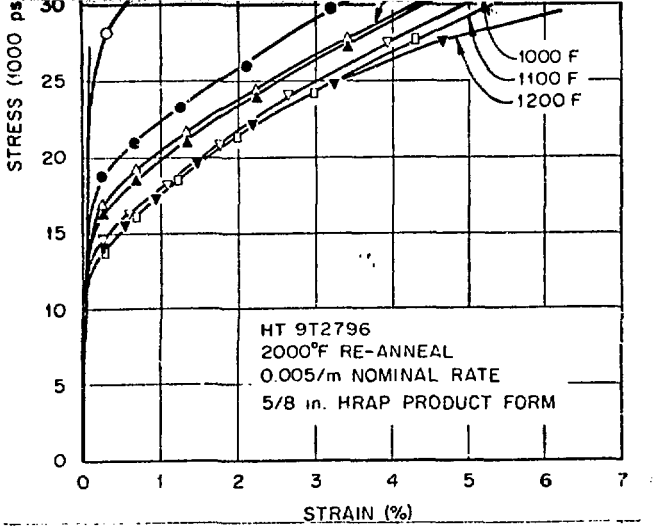

TYPE 304 STAINLESS STEEL, ANNEALED (HEAT 6043813)
ROOM TEMPERATURE
STRAIN RATE 0.005/min
STRAIN RANGE ≈ 0.9%

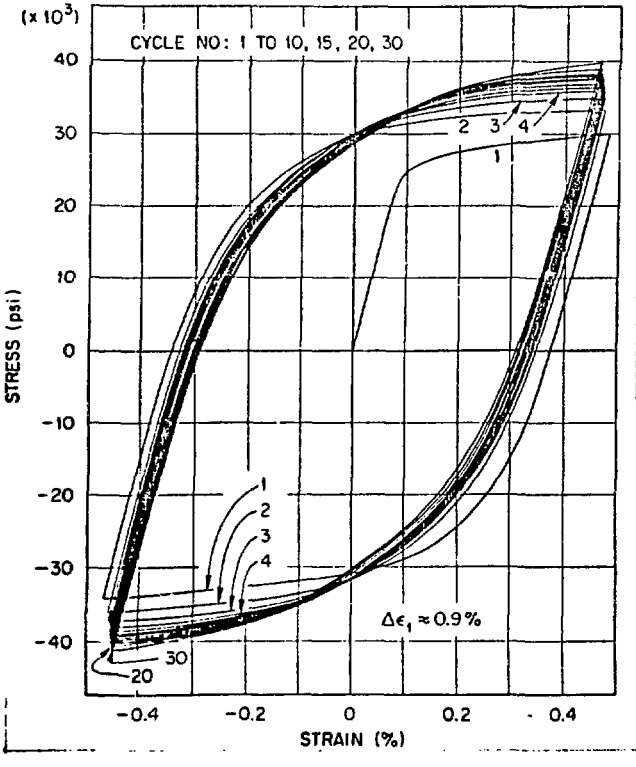

TYPE 304 STAINLESS STEEL, ANNEALED (HEAT 9T2796)
TEMPERATURE 1100°F
STRAIN RATE 0.005/min
STRAIN RANGE 1.0%

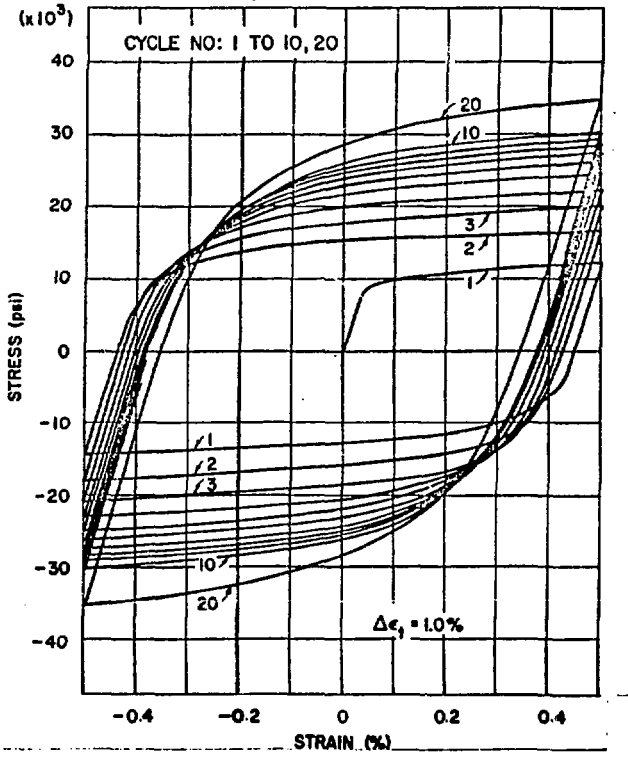

2

TYPE 304 S/S, ANNEALED (9T2796)
ROOM TEMPERATURE
SPECIMEN, C-9

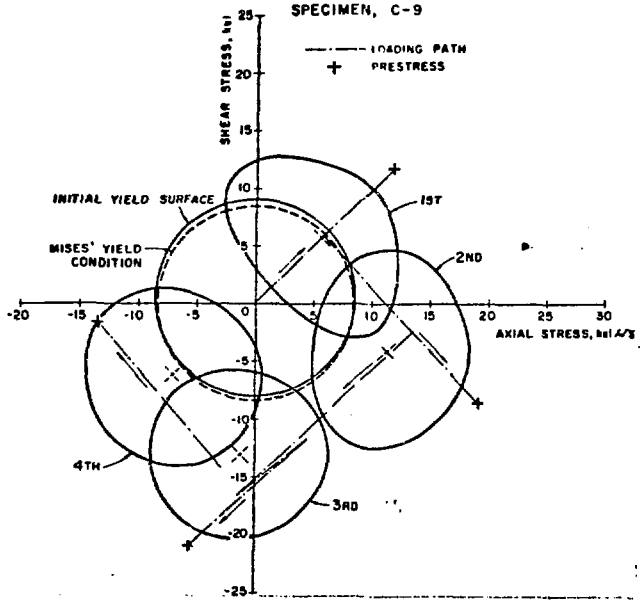

TYPE 304 SS, ANNEALED
HEAT NO. 9T2796
SPECIMEN C-10

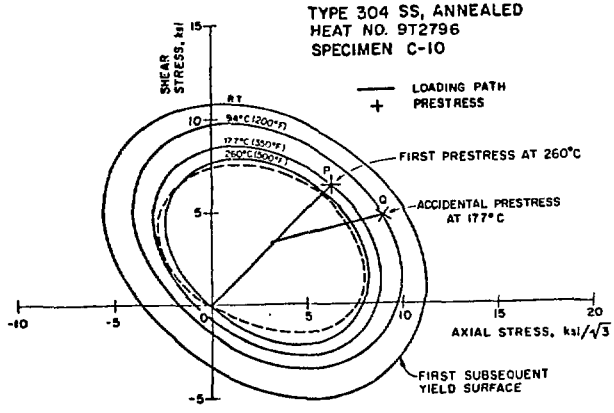

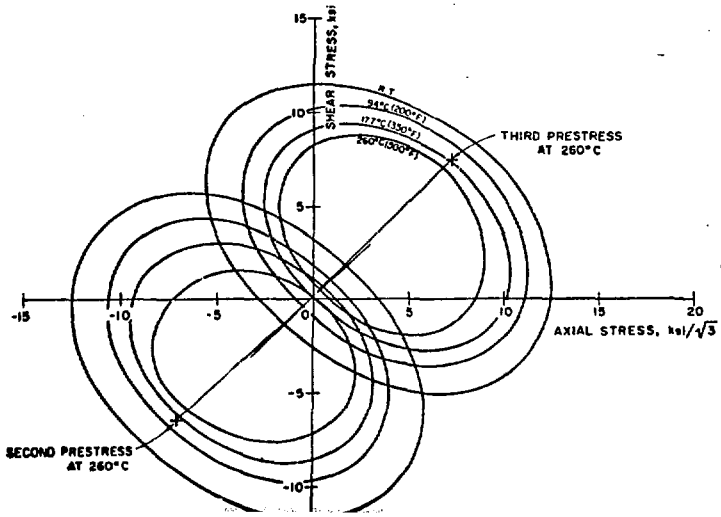

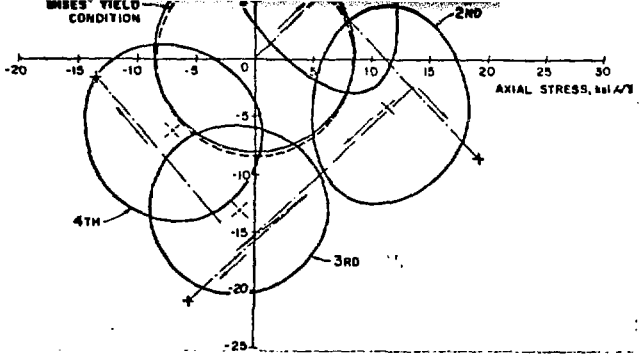
MISES' YIELD CONDITION
2ND
4TH
3RD
AXIAL STRESS, ksi

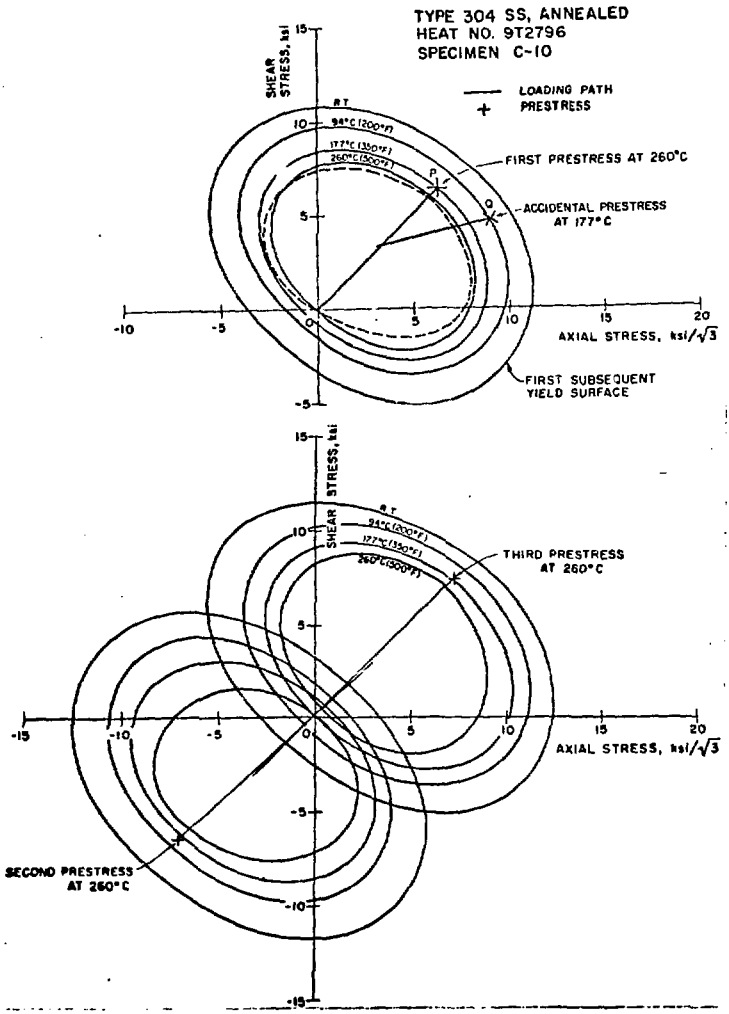
TYPE 304 SS, ANNEALED
HEAT NO. 9T2796
SPECIMEN C-10
LOADING PATH
PRESTRESS
SHEAR STRESS, ksi
R.T.
93°C (200°F)
177°C (350°F)
260°C (500°F)
FIRST PRESTRESS AT 260°C
ACCIDENTAL PRESTRESS AT 177°C
AXIAL STRESS, ksi/√3
FIRST SUBSEQUENT YIELD SURFACE
THIRD PRESTRESS AT 260°C
SECOND PRESTRESS AT 260°C

2

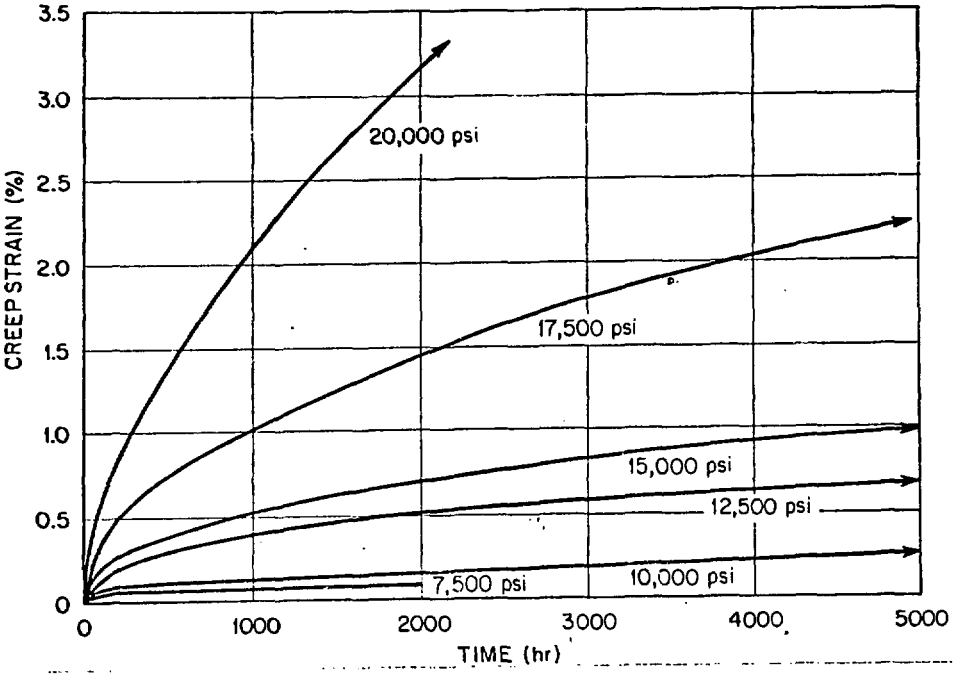
CREEP STRAIN (%)
TIME (hr)
20,000 psi
17,500 psi
15,000 psi
12,500 psi
10,000 psi
7,500 psi

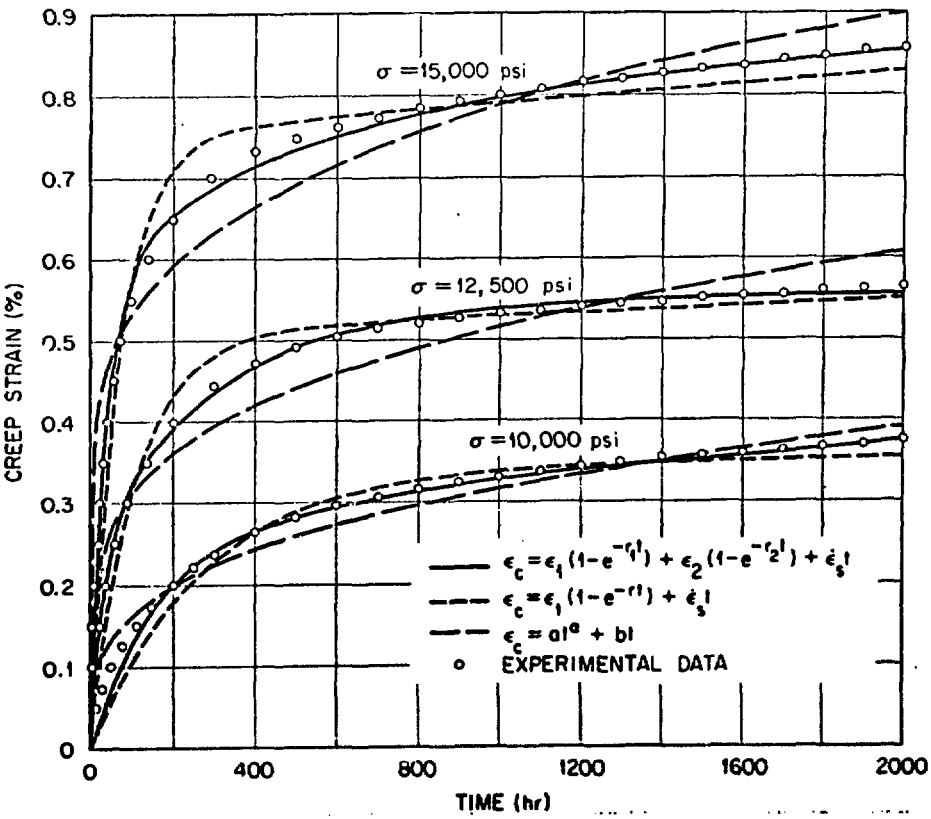
CREEP STRAIN (%)
TIME (hr)
σ =15,000 psi
σ =12,500 psi
σ =10,000 psi
$\epsilon_c = \epsilon_1(1-e^{-r_1 t}) + \epsilon_2(1-e^{-r_2 t}) + \dot{\epsilon}_s t$
$\epsilon_c = \epsilon_1(1-e^{-rt}) + \dot{\epsilon}_s t$
$\epsilon_c = at^a + bt$
EXPERIMENTAL DATA

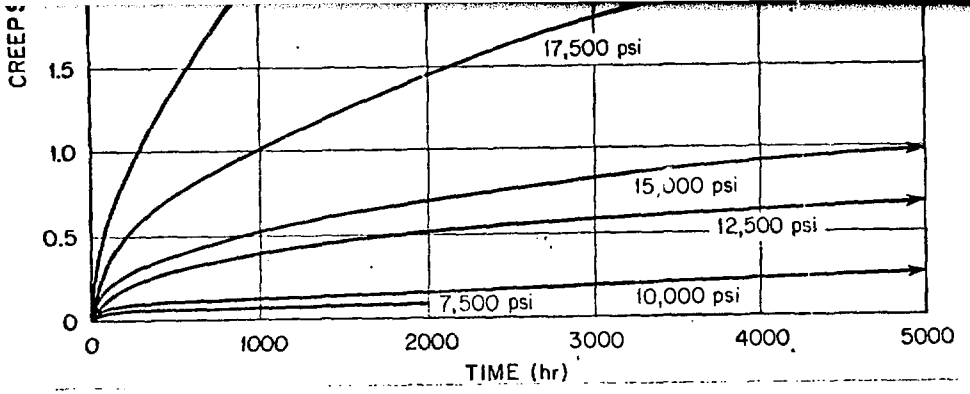
CREEP
1.5
1.0
0.5
0
17,500 psi
15,000 psi
12,500 psi
10,000 psi
7,500 psi
0
1000
2000
3000
4000
5000
TIME (hr)

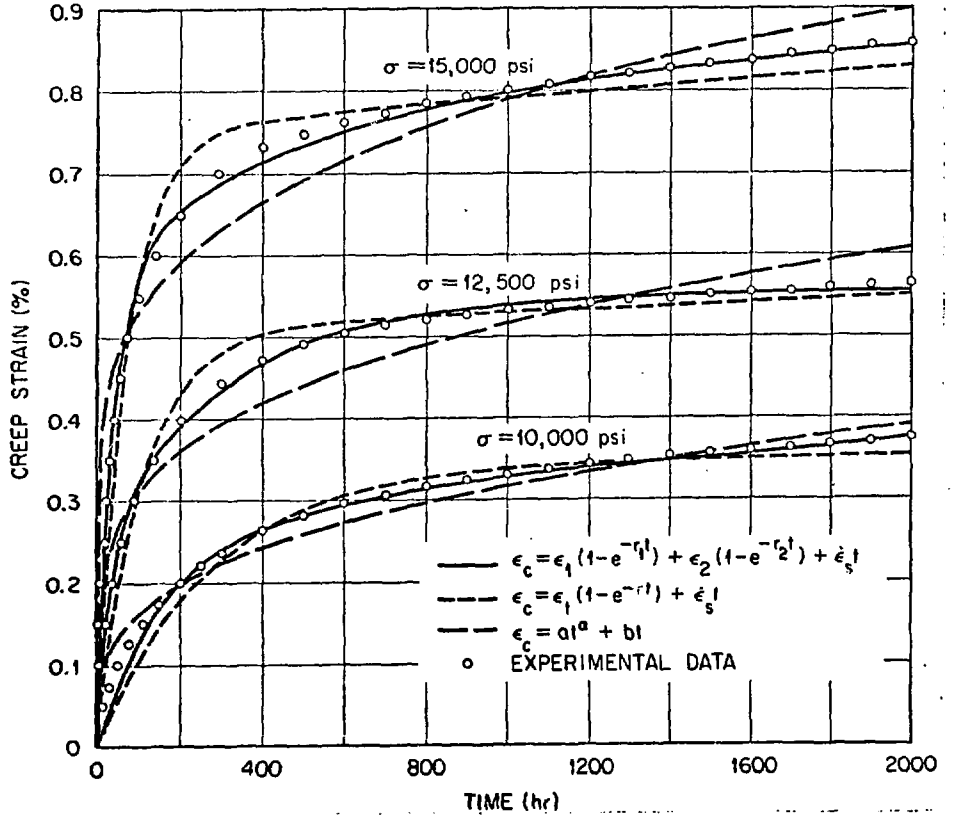
CREEP STRAIN (%)
0.9
0.8
0.7
0.6
0.5
0.4
0.3
0.2
0.1
0
σ = 15,000 psi
σ = 12,500 psi
σ = 10,000 psi
$\epsilon_c = \epsilon_1(1-e^{-r_1 t}) + \epsilon_2(1-e^{-r_2 t}) + \dot{\epsilon}_s t$
$\epsilon_c = \epsilon_1(1-e^{-rt}) + \dot{\epsilon}_s t$
$\epsilon_c = at^a + bt$
EXPERIMENTAL DATA
0
400
800
1200
1600
2000
TIME (hr)

2

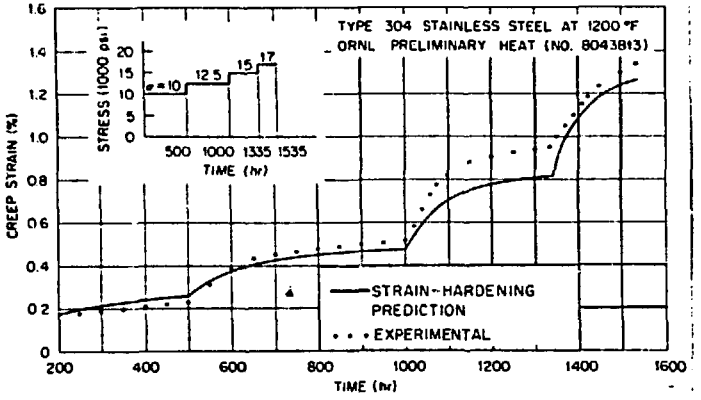
TYPE 304 STAINLESS STEEL AT 1200 °F
ORNL PRELIMINARY HEAT (NO. 8043B13)
STRESS (1000 psi)
σ = 10
12.5
15
17
500 1000 1335 1535
TIME (hr)
CREEP STRAIN (%)
STRAIN-HARDENING PREDICTION
EXPERIMENTAL
TIME (hr)

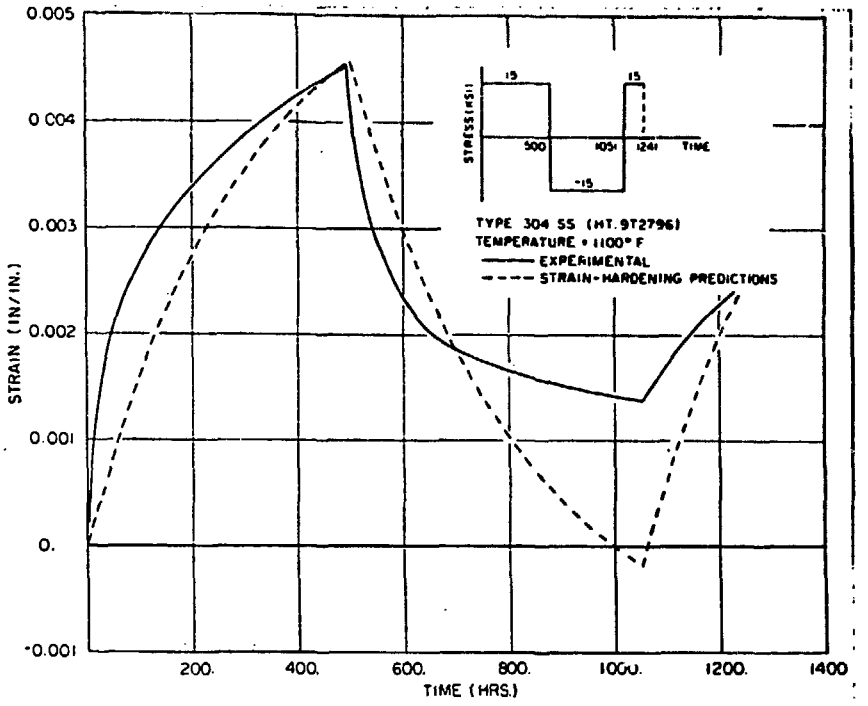
STRESS (ksi)
15
15
500
TIME
-15
TYPE 304 SS (HT. 9T2796)
TEMPERATURE = 1100° F
EXPERIMENTAL
STRAIN-HARDENING PREDICTIONS
STRAIN (IN/IN.)
TIME (HRS.)

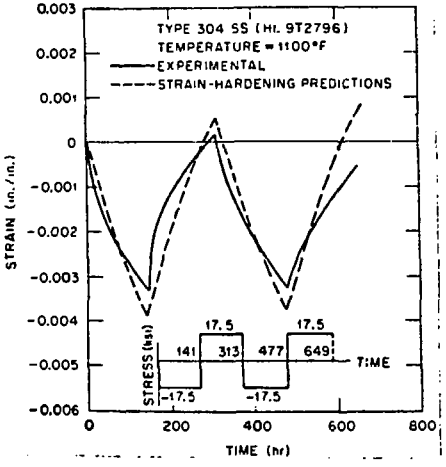
TYPE 304 SS (HT. 9T2796)
TEMPERATURE = 1100°F
EXPERIMENTAL
STRAIN-HARDENING PREDICTIONS
STRAIN (in./in.)
STRESS (ksi)
17.5
141
313
477
649
TIME
-17.5
-17.5
TIME (hr)

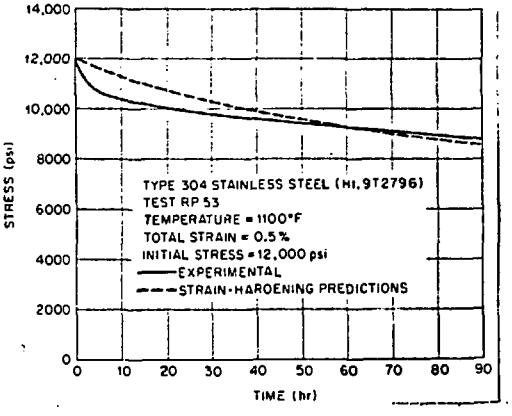
STRESS (psi)
TYPE 304 STAINLESS STEEL (HT. 9T2796)
TEST RP 53
TEMPERATURE = 1100°F
TOTAL STRAIN = 0.5 %
INITIAL STRESS = 12,000 psi
EXPERIMENTAL
STRAIN-HARDENING PREDICTIONS
TIME (hr)

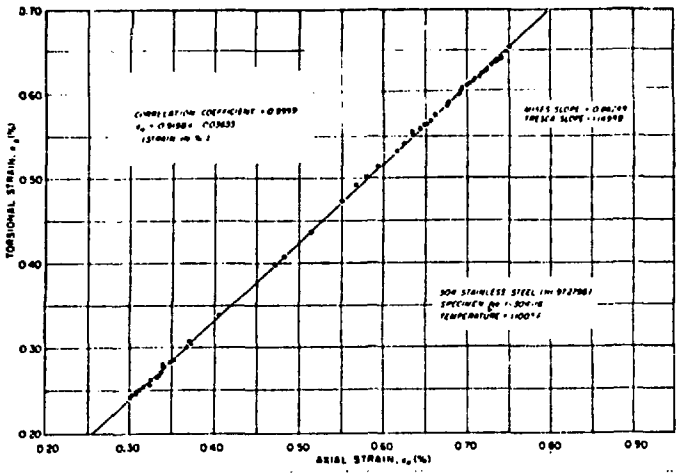
TORSIONAL STRAIN, ϵ_θ (%)
AXIAL STRAIN, ϵ_z (%)
0.20
0.30
0.40
0.50
0.60
0.70
0.80
0.90
304 STAINLESS STEEL (HT 972796)
TEMPERATURE = 1100°F

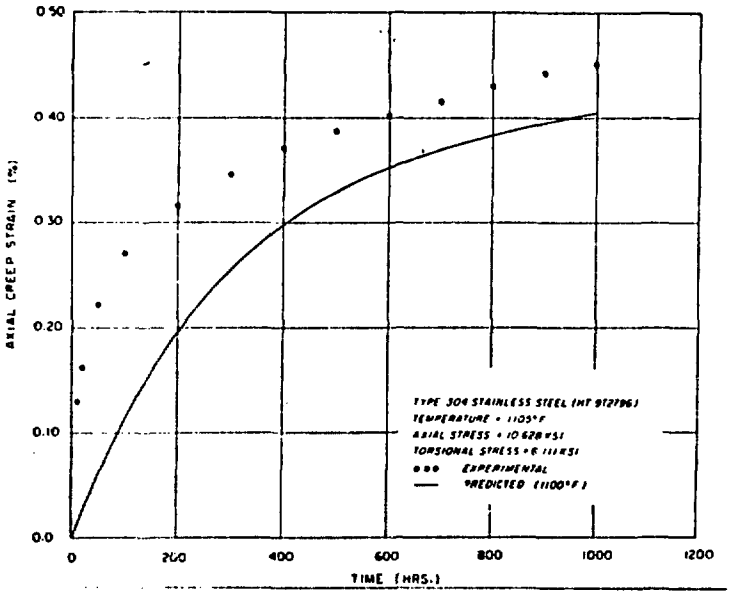
AXIAL CREEP STRAIN (%)
TIME (HRS.)
0.0
0.10
0.20
0.30
0.40
0.50
0
200
400
600
800
1000
1200
TYPE 304 STAINLESS STEEL (HT 972796)
TEMPERATURE = 1105°F
AXIAL STRESS = 10 628 PSI
TORSIONAL STRESS = 6 111 PSI
EXPERIMENTAL
PREDICTED (1100°F)

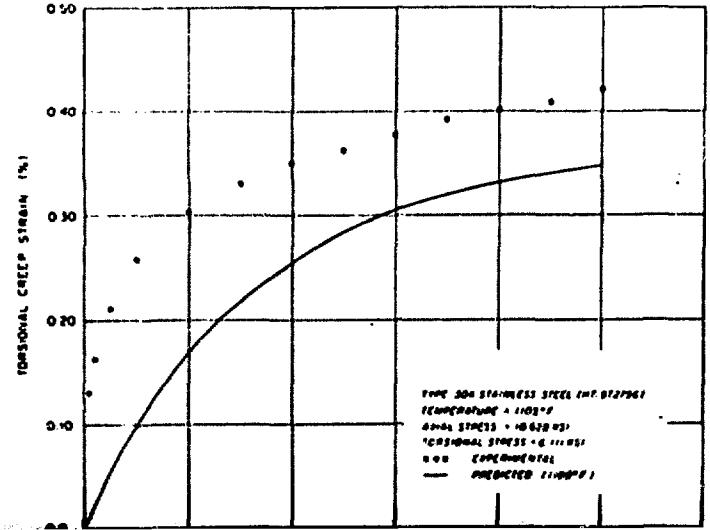
TORSIONAL CREEP STRAIN (%)
0.10
0.20
0.30
0.40
0.50
EXPERIMENTAL

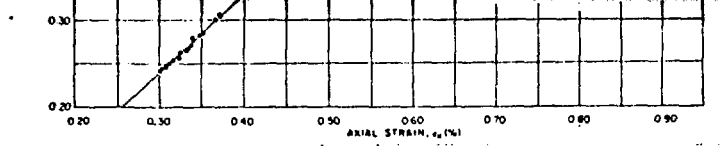
0.30
0.20
0.20
0.30
0.40
0.50
0.60
0.70
0.80
0.90
AXIAL STRAIN, ϵ_a (%)

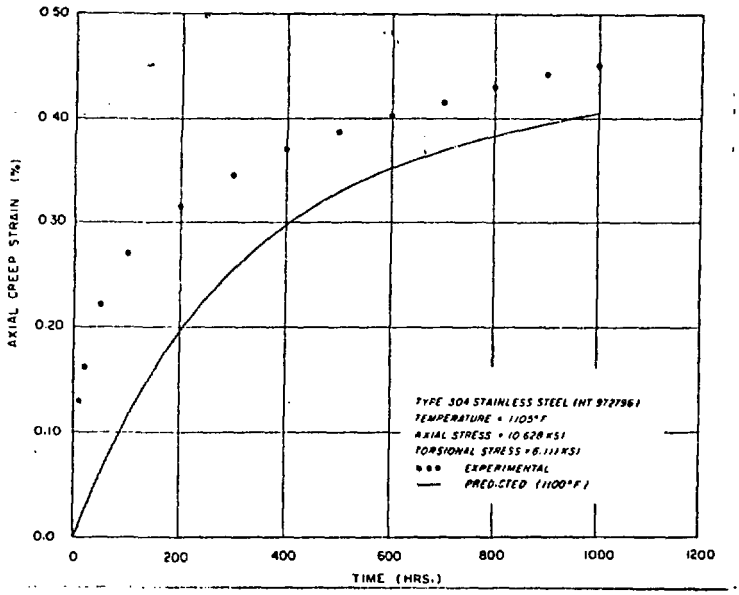
AXIAL CREEP STRAIN (%)
0.50
0.40
0.30
0.20
0.10
0.0
0
200
400
600
800
1000
1200
TIME (HRS.)
TYPE 304 STAINLESS STEEL (HT 972796)
TEMPERATURE = 1105°F
AXIAL STRESS = 10.628 KSI
TORSIONAL STRESS = 6.111 KSI
EXPERIMENTAL
PREDICTED (1100°F)

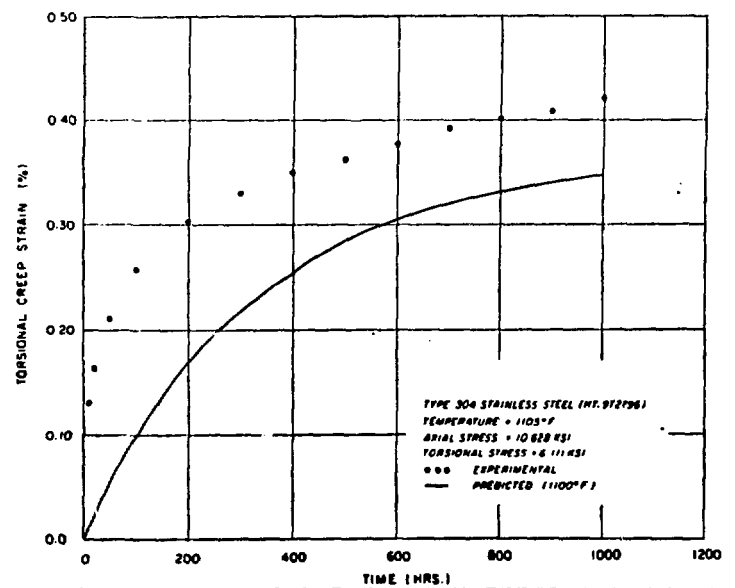
TORSIONAL CREEP STRAIN (%)
0.50
0.40
0.30
0.20
0.10
0.0
0
200
400
600
800
1000
1200
TIME (HRS.)
TYPE 304 STAINLESS STEEL (HT. 972796)
TEMPERATURE = 1105°F
AXIAL STRESS = 10.628 KSI
TORSIONAL STRESS = 6.111 KSI
EXPERIMENTAL
PREDICTED (1100°F)

2

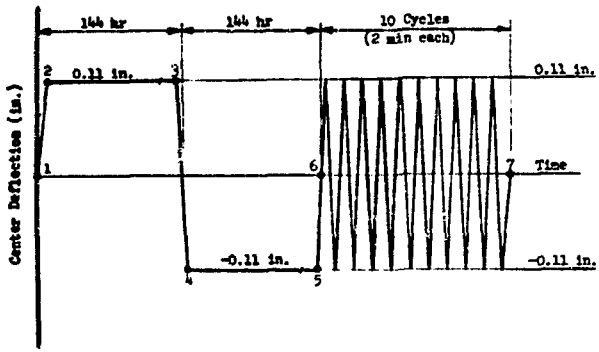
144 hr
144 hr
10 Cycles
(2 min each)
0.11 in.
0.11 in.
-0.11 in.
-0.11 in.
Time
Center Deflection (in.)
1
2
3
4
5
6
7

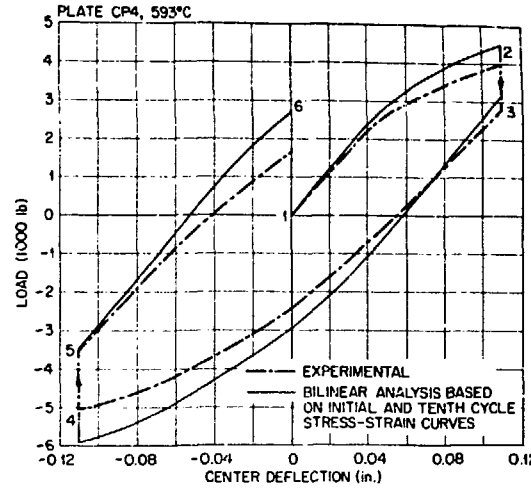
PLATE CP4, 593°C
LOAD (1000 lb)
CENTER DEFLECTION (in.)
EXPERIMENTAL
BILINEAR ANALYSIS BASED ON INITIAL AND TENTH CYCLE STRESS-STRAIN CURVES

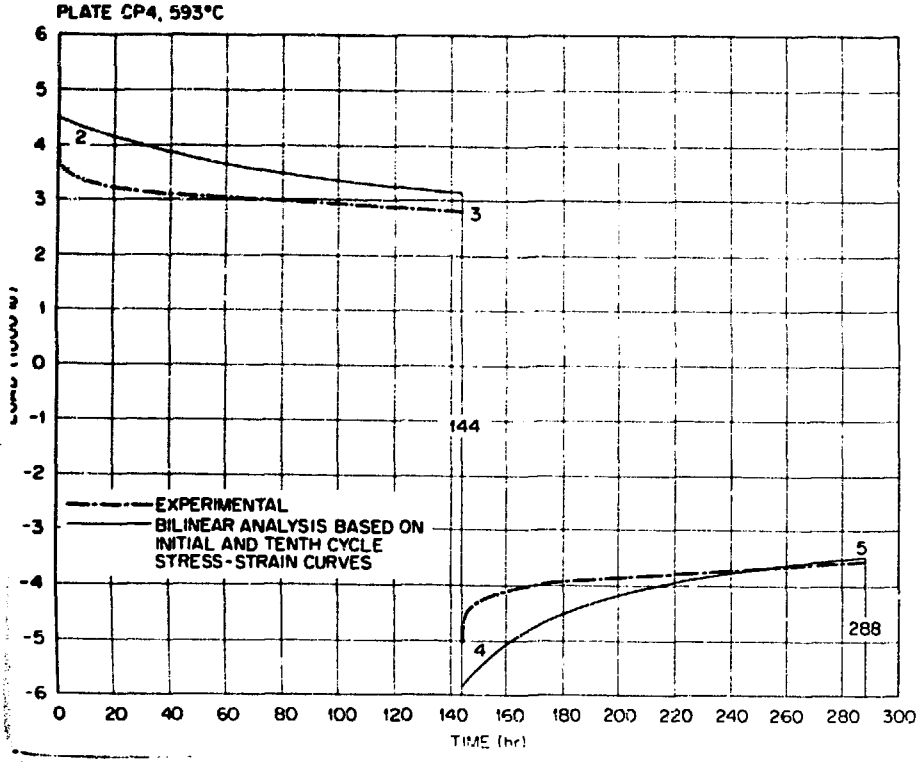
PLATE CP4, 593°C
TIME (hr)
144
288
EXPERIMENTAL
BILINEAR ANALYSIS BASED ON INITIAL AND TENTH CYCLE STRESS-STRAIN CURVES

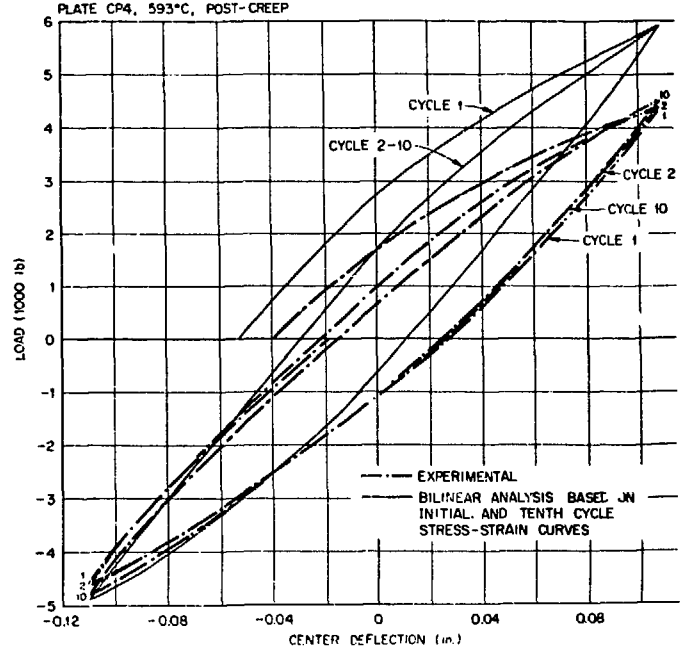
PLATE CP4, 593°C, POST-CREEP
CYCLE 1
CYCLE 2-10
CYCLE 2
CYCLE 10
CYCLE 1
LOAD (1000 lb)
CENTER DEFLECTION (in.)
EXPERIMENTAL
BILINEAR ANALYSIS BASED ON INITIAL AND TENTH CYCLE STRESS-STRAIN CURVES